PHYSICAL REVIEW D **80,** 101302(R) (2009)

Cosmic steps in modeling dark energy

Tower Wang*

Center for High-Energy Physics, Peking University, Beijing 100871, China

(Received 18 August 2009; published 17 November 2009)

Past and recent data analyses gave some hints of steps in dark energy. Considering dark energy as a dynamical scalar field, we investigate several models with various steps: a step in the scalar potential, a step in the kinetic term, a step in the energy density, and a step in the equation-of-state parameter w. These toy models provide a workable mechanism to generate steps and features of dark energy. Remarkably, a single real scalar can cross $w = -1$ dynamically with a step in the kinetic term.

DOI: 10.1103/PhysRevD.80.101302 PACS numbers: 95.36.+x

I. INTRODUCTION

Dark energy is a popular explanation for the recent acceleration of our Universe. In order to draw a portrait of dark energy, it is necessary to parameterize it and constrain the parameters from observational data. By the past and recent data analyses, it was indicated that the dark energy could have various steps in its parameters. Several years ago, a late-time transition in the equation of state (EOS) was studied by Bassett *et al.* [1]. Very recently, Huang *et al.* [2] reported that dark energy might spring out at a low redshift. However, there were few theoretical studies to explain such steps in the EOS or in the density of dark energy.

Our purpose here is to make a step toward this direction. We will treat dark energy as a dynamical scalar field, and then study a step in the scalar potential, in the kinetic term, in the energy density, and in the EOS, respectively. Lacking enough observational data, hitherto the portrait of dark energy is still vague and the hints of steps are weak, so we do not attempt to build a realistic model in this paper. Instead, to give a vivid picture of the mechanism, we will play with simplified toy models and choose exaggerated model parameters. Because these models are difficult to solve analytically, for the most part we will rely on numerical algorithms. The models and algorithms can be easily extended and refined to give a more realistic description of dark energy.

Although this could be the first time to systematically study cosmic steps in dark energy models with an explicit Lagrangian, the stepped model is not novel in cosmology. It is an old story: possibly steps of the inflaton potential have left some fingerprints at the birth of our Universe [3]. Since the dark energy is more elusive, the physical origin of the stepped dark energy field is less clear than the stepped inflaton field.

II. METHODOLOGY

Before going to specific models, we will describe the general framework and numerical methods in some detail. Impatient readers can skip directly to the next section to get our models (10), (13), and (20) and main results depicted in figures.

In the absence of spatial fluctuations, the Lagrangian density of a scalar field minimally coupled to gravity has the form

$$\mathcal{L}_\phi = a^3\left[\frac{1}{2}f(\phi)\dot{\phi}^2 - V(\phi)\right], \tag{1}$$

where a is the scale factor. Here the function $f(\phi)$ in the kinetic term is new. It is positive for quintessence [4] and negative for phantom [5]. Later on we will also discuss a new model in which $f(\phi)$ evolves dynamically from $+1$ to -1. In that situation, the single real scalar plays the role of quintom [6].

In a flat universe dominated by dark energy together with cold dark matter, if we ignore the contribution of ordinary matter for simplicity, then the evolution dynamics is governed by the following Friedmann equations:

$$\begin{aligned} H^2 &= \frac{8\pi G_N}{3}(\rho_m + \rho) \\ &= \frac{8\pi G_N}{3}\left[\frac{\rho_{m0}a_0^3}{a^3} + \frac{1}{2}f(\phi)\dot{\phi}^2 + V(\phi)\right], \end{aligned} \tag{2}$$

$$\begin{aligned} \dot{H} &= -4\pi G_N(\rho_m + \rho + p) \\ &= -4\pi G_N\left[\frac{\rho_{m0}a_0^3}{a^3} + f(\phi)\dot{\phi}^2\right]. \end{aligned} \tag{3}$$

Here ρ_m is the energy density of dark matter, taking value ρ_{m0} at the present time with the scale factor $a = a_0$. The dark energy ϕ has an energy density ρ and a pressure p, whose subscripts have been left out for briefness. One should not mistake ρ and p as the total energy density and the total pressure. The EOS parameter is defined by $w = p/\rho$ as usual.

In the above we have used a dot to denote the derivative with respect to comoving (physical) time t. For instance, we have taken the convention of notation $\dot{\phi} = d\phi/dt$ and defined $H = \dot{a}/a$. It will be convenient to employ the notations $x = \ln(a/a_0) = -\ln(1+z)$ and $\phi' = d\phi/dx$,

*wangtao218@pku.edu.cn

then they give us a useful relation $\dot{\phi} = H\phi' = -H(1+z)\phi_{,z}$. Utilizing (2), we find the kinetic energy is

$$\frac{1}{2}f\dot{\phi}^2 = \frac{8\pi G_N f[\rho_{m0}(1+z)^3 + V](1+z)^2\phi_{,z}^2}{6 - 8\pi G_N f(1+z)^2\phi_{,z}^2}. \quad (4)$$

The equation of motion

$$f\ddot{\phi} + 3Hf\dot{\phi} + \frac{1}{2}f_{,\phi}\dot{\phi}^2 + V_{,\phi} = 0 \quad (5)$$

for the scalar field can be written as

$$\begin{aligned} &4\pi G_N f(1+z)[\rho_{m0}(1+z)^3 + 4V]\phi_{,z} \\ &= 8\pi G_N f(1+z)^2[\rho_{m0}(1+z)^3 + V]\phi_{,zz} \\ &\quad + 16\pi^2 G_N^2 f^2(1+z)^3[\rho_{m0}(1+z)^3 + 2V]\phi_{,z}^3 \\ &\quad + 4\pi G_N f_{,\phi}(1+z)^2[\rho_{m0}(1+z)^3 + V]\phi_{,z}^2 \\ &\quad + V_{,\phi}[3 - 4\pi G_N f(1+z)^2\phi_{,z}^2]. \end{aligned} \quad (6)$$

Given the explicit form of $f(\phi)$ and $V(\phi)$, Eq. (6) alone dictates the evolution of dark energy. But this is a highly nonlinear second order differential equation. In most cases we have to resort to numerical methods. We will take two slightly different schemes, dubbed the linear iteration method and the cubic iteration method, since they reform Eq. (6) into linear algebraic equations or cubic algebraic equations, respectively. Let us elaborate on them now.

For numerically evolving Eq. (6) from an initial point z_i to the final point z_f, we partition the interval $[z_i, z_f]$ into N equal subintervals of width $h = z_j - z_{j-1} = (z_f - z_i)/N$. It is convenient to notate $\phi_j = \phi(z_j)$ for short, where $j = 0, 1, 2, \ldots, N$. For numerical computation, the derivatives can be approximated by finite differences

$$\left.\frac{d\phi}{dz}\right|_{z=z_j} = \frac{\phi_{j+1} - \phi_{j-1}}{2h}, \quad (7)$$

$$\left.\frac{d^2\phi}{dz^2}\right|_{z=z_j} = \frac{\phi_{j+2} - 2\phi_j + \phi_{j-2}}{4h^2}. \quad (8)$$

Making use of approximations (7) and (8), one can recast Eq. (6) into a linear algebraic equation with respect to ϕ_{j+2}. Starting with the initial values of ϕ_j at $j = 0, 1, 2, 3$, we can get the values of all ϕ_j with $j > 3$ iteratively. The linear iteration method gives a unique path of ϕ for numerical evolutions. Its disadvantage is the excessive number of initial conditions. Remember that for a second order differential equation we usually impose two initial conditions. In practical operation, we treat with potentials flat at the initial point ϕ_i, and set $\phi_0 = \phi_1 = \phi_2 = \phi_3 = \phi_i$.

Rather than (8) one may tend to estimate the second order derivative with

$$\left.\frac{d^2\phi}{dz^2}\right|_{z=z_j} = \frac{\phi_{j+1} - 2\phi_j + \phi_{j-1}}{h^2}. \quad (9)$$

Now we need only two initial conditions, for instance, $\phi_0 = \phi_1 = \phi_i$. This is the starting point of the cubic iteration scheme. In such a scheme, instead of a linear equation of ϕ_{j+2}, one has to solve a cubic equation with respect to ϕ_{j+1}. The formula of roots of a cubic equation is well known. For our purpose, it is enough to treat them in two general categories: (i) if the equation has one real root and a pair of imaginary roots, then ϕ_{j+1} takes a value of the real root; (ii) if all roots are real, we determine the value of ϕ_{j+1} by minimizing $|\phi_{j+1} - \phi_j|$. The trick enables us to pick out the smoothest evolution path of ϕ, and fortunately this path is unique in our simulation. Even if the path is not unique after applying the above trick, one can still find the smoothest path by further minimizing $|\phi_{j+1} + \phi_{j-1} - 2\phi_j|$, etc.

The above two methods are operated independently in our algorithms. As double checks, they agree with each other very well. In fact, the resulting graphs look like duplicates. During the numerical simulation, we define the reduced Planck mass $M_{\rm pl} = 1/\sqrt{8\pi G_N}$, the fractional density of dark energy $\Omega_{\rm DE} = \rho_{\rm DE}/(3M_p^2H^2)$ and the present fractional density of dark matter $\Omega_{m0} = \rho_{m0}/(3M_p^2H_0^2)$, where H_0 is Hubble parameter at the present time. Moreover, we set $\Omega_{m0} = 0.3$ and work in the unit $M_{\rm pl} = 1$. In a flat universe, ignoring the contribution of ordinary matter, one has $\Omega_{\rm DE} + \Omega_m = 1$. For every specific model below, we evolve Eq. (6) from $z_i = 20$ to $z_f = 0$ with $N = 2000$ subintervals. Fixing the initial conditions and other parameters, if we increase either N or z_i, the change in results is unobservable. This confirms the reliability of our methods above and results below.

III. MODELS WITH STEPS

A. Steps in the scalar potential

So far we have not specified our models. It will be done in this section. First, suppose the potential of dark energy is broadly flat but has a sudden transition near $\phi = b$. Then it is natural to model such a stepped potential in the following form:

$$V(\phi) = V_0\left[1 + c\tanh\left(\frac{\phi - b}{d}\right)\right]. \quad (10)$$

For relatively small d, the hyperbolic tangent function is a good smooth analytic approximation to a step function. The parameter b determines the location of step in field space, while c and d control the height and width of step, respectively. Based on this model, more complicated ones can be obtained by superposing the steps or replacing the constant V_0 with other functions. Note here c is a dimensionless parameter, but b and d are in unit of reduced Planck mass $M_{\rm pl} = 1/\sqrt{8\pi G_N}$. However, in our simulation and figures, we will simply set $M_{\rm pl} = 1$.

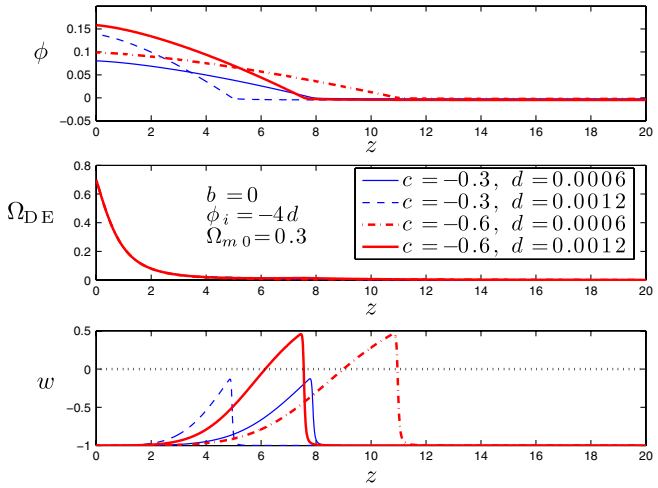

FIG. 1 (color online). Evolution curves of the quintessence field with potential (10) and $f = +1$. There are bumps in the curves of fractional density and EOS parameter, although the bump in fractional density is almost unnoticeable. The amplitude and location of bumps can be tuned by changing parameters in our model. We set $8\pi G_N = 1$ in all figures.

We study this potential in the context of quintessence with $f = +1$ and phantom with $f = -1$, respectively. Since $\Omega_{\rm DE0} + \Omega_{m0} = 1$ in a flat universe with negligible ordinary matter, it is easy to prove $V_0 = 3H_0^2(1 - \Omega_{m0})/(1 \pm |c|)$ for quintessence (lower sign) and phantom (upper sign). The simulation results for stepped quintessence are shown in Figs. 1 and 2. The results for phantom are depicted in Fig. 3. In plotting them we have chosen the step location $b = 0$, and the initial value of ϕ is chosen as $\phi_i = -4d$ at redshift $z_i = 20$. From the figures we can see

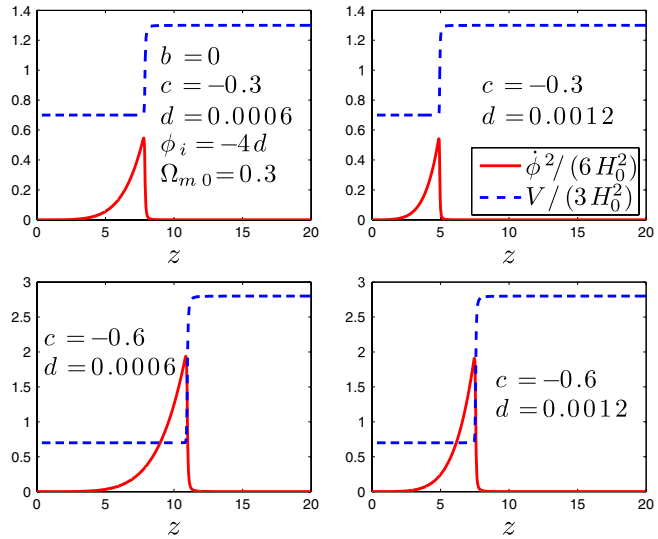

FIG. 2 (color online). The rise and fall of the kinetic energy and potential of a stepped quintessence with potential (10) and $f = +1$. Both the kinetic energy and the potential are normalized by $3H_0^2$, where H_0 is the Hubble parameter at $z = 0$.

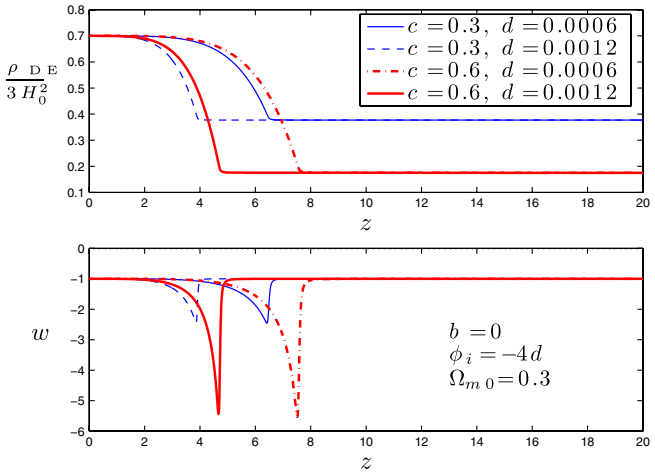

FIG. 3 (color online). For stepped phantom with potential (10) and $f = -1$. The dark energy density climbs up a step, while EOS parameter has a dip nearby. Similarly to the stepped quintessence, the amplitude and location of the steps and dips are tunable as we change the model parameters.

a step in the energy density. Quintessence falls down the step but phantom climbs up. Although the location of step in field space is fixed by $b = 0$, its location in redshift space is dependent of c and d. At the same location there is a feature (a bump for quintessence or a dip for phantom) in curves of kinetic energy and EOS parameter. Amplitudes of steps and features are determined mainly by parameter c. The initial value ϕ_i of the scalar field resides well in the flat region of the potential because $\tanh(-4) \simeq -0.999$. If we increase the absolute value of ϕ_i, the steps and features will shift to lower redshift region.

From Figs. 2 and 3, one can roughly read the location z_T and width Δ_T of the step as well as the initial density ρ_i and final density ρ_f of the dark energy. In data analysis, it is useful to capture these properties by parameterizing the dark energy density as

$$\rho = \rho_i + \frac{\rho_f - \rho_i}{1 + \exp(\frac{z - z_T}{\Delta_T})} = \frac{\rho_i + \rho_f}{2} + \frac{\rho_i - \rho_f}{2} \tanh\left(\frac{z - z_T}{2\Delta_T}\right). \quad (11)$$

This parametrization is applicable when the dark energy changes from ρ_i to ρ_f near the redshift z_T. Assuming the dark energy is decoupled with other ingredients, we have the continuity equation $\dot\rho + 3H(\rho + p) = 0$ or equivalently $(\ln\rho)' = -3(1 + w)$. Corresponding to (11), it gives

$$w = \frac{(1 + z)(\rho_i - \rho_f)\exp(\frac{z - z_T}{\Delta_T})}{3\Delta_T[1 + \exp(\frac{z - z_T}{\Delta_T})][\rho_f + \rho_i \exp(\frac{z - z_T}{\Delta_T})]} - 1. \quad (12)$$

One may check that the function gives rise to a bump if $\rho_i > \rho_f$ or a dip when $\rho_i < \rho_f$, in agreement with Figs. 1 and 3.

B. Steps in the kinetic term

Having explored the steps in dark energy potential, we discuss what will happen if there is a step in the coefficient $f(\phi)$ of the kinetic term. It is interesting to study a new model

$$f(\phi) = c\tanh\left(\frac{\phi - b}{d}\right), \qquad V(\phi) = V_0\left[1 + \tanh\left(\frac{\phi^2}{q^2}\right)\right]. \tag{13}$$

In favor of the fact that $\Omega_{\rm DE0} + \Omega_{m0} = 1$, we can set $V_0 = 3H_0^2(1 - \Omega_{m0})/2$. In the potential $V(\phi)$ there is a deep dip, whose depth has been fixed. The coefficient $f(\phi)$ is nontrivial. It has a step located at $\phi = b$ with amplitude c and width d. Again c is a dimensionless parameter, while b and d are in unit of reduced Planck mass $M_{\rm pl}$. As mentioned before, we set $M_{\rm pl} = 1$ in our simulation and figures.

The idea is to settle the potential bottom $\phi = 0$ in the region $f > 0$ by ensuring $c\tanh(-b/d) > 0$. Given an appropriate initial condition, the scalar first rolls down to the bottom of potential and then moves up, getting closer and closer to the point $\phi = b$. However, this model still requires some fine-tuning, because it is not always possible for the scalar field to pass the sign-inversion point of $f(\phi)$ after leaving the bottom of potential. We fine-tune the parameters, and then numerically evolve the equation of motion (6). According to the simulation results in Fig. 4, both the density and the EOS parameter of dark energy decrease near the sign-inversion point. In particular, the EOS parameter jumps down abruptly from $w > -1$ to $w \ll -1$. This is a simple way to cross the EOS barrier $w = -1$. To make it we need only one real scalar field, completely relying on its own dynamics. However, one

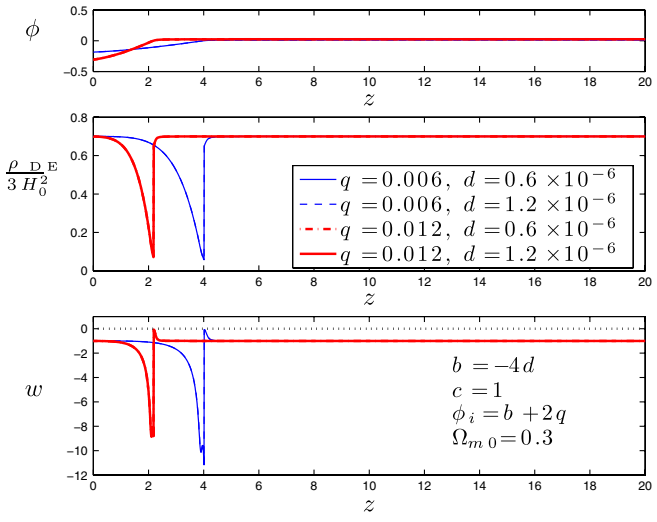

FIG. 4 (color online). The evolution of the scalar field, dark energy density and EOS parameter for the stepped quintom model (13). In contrast with previous figures, a small change in parameter d does not modify the evolution curves significantly.

should not regard (13) as more than a toy model. There is an infamous instability in any model with a wrong-signed kinetic term, e.g., in the phantom model [5]. We suspect the stepped quintom model here suffers from the same problem. Various issues on this class of model were explored in [7–9].

C. Steps in the EOS parameter

If there is a step in the EOS parameter, one usually parameterizes w in a form [1] similar to (11). However, for building a model later, we parameterize it in an alternative way,

$$w = w_i + \frac{w_f - w_i}{1 + (\frac{1+z}{1+z_T})^\lambda} = w_i + \frac{w_f - w_i}{1 + (\frac{a_T}{a})^\lambda}, \tag{14}$$

where $\lambda \gg 1$. With this form, the continuity equation can be integrated out as

$$\begin{aligned}\rho &= \rho_T\left(\frac{a_T}{a}\right)^{3(1+w_i)}\left[\frac{1}{2} + \frac{1}{2}\left(\frac{a}{a_T}\right)^\lambda\right]^{3(w_i - w_f)/\lambda} \\ &= \rho_T\left(\frac{a_T}{a}\right)^{3(1+w_f)}\left[\frac{1}{2} + \frac{1}{2}\left(\frac{a_T}{a}\right)^\lambda\right]^{3(w_i - w_f)/\lambda}.\end{aligned} \tag{15}$$

Note there is a duality $w_i \leftrightarrow w_f$, $\lambda \leftrightarrow -\lambda$ in (14). We are most interested in the following special cases:

(i) $w_i = -1$; Now the EOS takes the form

$$\frac{p}{\rho} = w_f - \frac{1 + w_f}{2}\left(\frac{\rho}{\rho_T}\right)^{\lambda/[3(1+w_f)]}. \tag{16}$$

(ii) $w_f = -1$. In this case, we reexpress the EOS as

$$\frac{p}{\rho} = w_i - \frac{1 + w_i}{2}\left(\frac{\rho_T}{\rho}\right)^{\lambda/[3(1+w_i)]}. \tag{17}$$

The equations of state (16) and (17) can be cast into a unified form

$$p = \rho(w_c - A\rho^\alpha), \tag{18}$$

from which one can integrate the continuity equation to give

$$\rho^\alpha = \frac{1 + w_c}{A + Ba^{3\alpha(1+w_c)}} = \frac{1 + w_c}{A[1 + (\frac{a}{a_T})^{3\alpha(1+w_c)}]}. \tag{19}$$

It is time for us to reconstruct the potential in accordance with (1) and (14). This is accomplishable if the Universe is exclusively dominated by the scalar field ϕ. To do this, we assume $f(\phi)$ is a nonzero constant and $\rho_m = 0$, $w_c \neq -1$. For details on reconstructing the potential of scalar dark energy, please refer to [10–13]. Making use of Eqs. (2), (3), (18), and (19), we finally obtain

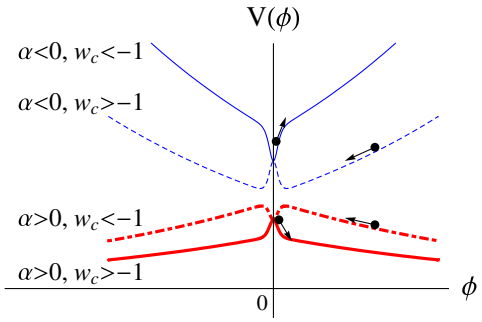

FIG. 5 (color online). A rough illustration of potential (20) with different parameter choices. The arrows indicate evolving directions of the dark energy field. For example, when $\alpha < 0$ and $w_c < -1$, the potential is illustrated by the thin solid (blue) line, and the scalar field rolls up the potential from the bottom $\phi = 0$ to $\phi \to \pm\infty$, while the EOS parameter w evolves from -1 to w_c asymptotically. The dashed (blue) line corresponds to the potential with $\alpha < 0$ and $w_c > -1$, in which case the scalar field rolls down the potential from $\phi \to \pm\infty$ to one of the local minimum point, and the EOS parameter w evolves form w_c to -1.

$$a^{3\alpha(1+w_c)} = \frac{A}{B}\sinh^2\left(\frac{\phi}{\phi_c}\right),$$
$$V(\phi) = \frac{V_c}{2}\cosh^{-2/\alpha}\left(\frac{\phi}{\phi_c}\right)\left[2 - (1+w_c)\tanh^2\left(\frac{\phi}{\phi_c}\right)\right] \tag{20}$$

with $\phi_c^{-1} = \alpha\sqrt{6\pi G_N f(1+w_c)}$ and $V_c = [(1+w_c)/A]^{1/\alpha}$. For various choices of parameters, the shape of this potential is illustrated in Fig. 5. The EOS parameter $w \to w_c$ asymptotically as $\phi \to \pm\infty$. Near the bottom or top of the potential, it approaches -1. The field rolls down the potential as a quintessence if $w_c > -1$, but rolls up as a phantom when $w_c < -1$. We impose $|3\alpha(1+w_c)| \gg 1$ by hand to accomplish the sudden EOS transition (14).

IV. DISCUSSION

Treating dark energy as a scalar field, we explicitly modeled steps in its potential, kinetic term, density, and EOS, and thus provided a workable mechanism to explain the previously and recently claimed dark energy transitions. To arrive at a realistic model, more experimental and theoretical efforts are needed in the future. When this work was near completion, a related paper [14] appeared, where they arrived at models with an implicit potential similar to the shape of $V(\phi)$ in (13). As a partial list, some previous papers relevant to our work are [15–21].

ACKNOWLEDGMENTS

This work is supported by the China Postdoctoral Science Foundation. We are grateful to Tong Li and Wei Liao for discussions, and Qinyan Tan for help with programming.

[1] B. A. Bassett, M. Kunz, J. Silk, and C. Ungarelli, Mon. Not. R. Astron. Soc. **336**, 1217 (2002).
[2] Q. G. Huang, M. Li, X. D. Li, and S. Wang, Phys. Rev. D **80**, 083515 (2009).
[3] J. A. Adams, B. Cresswell, and R. Easther, Phys. Rev. D **64**, 123514 (2001).
[4] I. Zlatev, L. M. Wang, and P. J. Steinhardt, Phys. Rev. Lett. **82**, 896 (1999).
[5] R. R. Caldwell, Phys. Lett. B **545**, 23 (2002).
[6] B. Feng, X. L. Wang, and X. M. Zhang, Phys. Lett. B **607**, 35 (2005).
[7] A. Vikman, Phys. Rev. D **71**, 023515 (2005).
[8] S. Nojiri and S. D. Odintsov, Gen. Relativ. Gravit. **38**, 1285 (2006).
[9] J. Q. Xia, Y. F. Cai, T. T. Qiu, G. B. Zhao, and X. Zhang, Int. J. Mod. Phys. D **17**, 1229 (2008).
[10] T. D. Saini, S. Raychaudhury, V. Sahni, and A. A. Starobinsky, Phys. Rev. Lett. **85**, 1162 (2000).
[11] V. Sahni and A. Starobinsky, Int. J. Mod. Phys. D **15**, 2105 (2006).
[12] S. Capozziello, S. Nojiri, and S. D. Odintsov, Phys. Lett. B **632**, 597 (2006).
[13] E. Elizalde, S. Nojiri, S. D. Odintsov, D. Saez-Gomez, and V. Faraoni, Phys. Rev. D **77**, 106005 (2008).
[14] M. J. Mortonson, W. Hu, and D. Huterer, Phys. Rev. D **80**, 067301 (2009).
[15] S. Y. Zhou, Phys. Lett. B **660**, 7 (2008).
[16] S. Capozziello, S. Nojiri, and S. D. Odintsov, Phys. Lett. B **634**, 93 (2006).
[17] S. Nojiri and S. D. Odintsov, Phys. Lett. B **637**, 139 (2006).
[18] S. Nojiri, S. D. Odintsov, and H. Stefancic, Phys. Rev. D **74**, 086009 (2006).
[19] S. Nojiri, S. D. Odintsov, and S. Tsujikawa, Phys. Rev. D **71**, 063004 (2005).
[20] M. Szydlowski, O. Hrycyna, and A. Krawiec, J. Cosmol. Astropart. Phys. 06 (2007) 010.
[21] O. Hrycyna and M. Szydlowski, arXiv:0906.0335.